Hindawi Publishing Corporation
International Journal of Photoenergy
Volume 2012, Article ID 263254, 6 pages
doi:10.1155/2012/263254

Research Article

Silver Orthophosphate Immobilized on Flaky Layered Double Hydroxides as the Visible-Light-Driven Photocatalysts

Xianlu Cui,[1] Yaogang Li,[2] Qinghong Zhang,[2] and Hongzhi Wang[1]

[1] *State Key Laboratory for Modification of Chemical Fibers and Polymer Materials, Donghua University, Shanghai 201620, China*
[2] *Engineering Research Center of Advanced Glasses Manufacturing Technology, MOE, Donghua University, Shanghai 201620, China*

Correspondence should be addressed to Qinghong Zhang, zhangqh@dhu.edu.cn and Hongzhi Wang, wanghz@dhu.edu.cn

Received 15 July 2011; Accepted 19 September 2011

Academic Editor: Jinlong Zhang

Flaky layered double hydroxide (FLDH) was prepared by the reconstruction of its oxide in alkali solution. The composites with FLDH/Ag_3PO_4 mass ratios at 1.6 : 1 and 3 : 1 were fabricated by the coprecipitation method. The powders were characterized by X-ray diffraction, field-emission scanning electron microscopy, transmission electron microscope, and UV-vis diffuse reflectance spectroscopy. The results indicated that the well-distributed Ag_3PO_4 in a fine crystallite size was formed on the surface of FLDH. The photocatalytic activities of the Ag_3PO_4 immobilized on FLDH were significantly enhanced for the degradation of acid red G under visible light irradiation compared to bare Ag_3PO_4. The composite with the FLDH/Ag_3PO_4 mass ratio of 3 : 1 showed a higher photocatalytic efficiency.

1. Introduction

The treatment of environmental pollutants in waste water by active semiconductor photocatalysts has recently attracted considerable attention for its ability to completely oxidize organic contaminants to carbon dioxide, water, and mineral acids [1–5]. Among the semiconductor photocatalysts, TiO_2 has been extensively studied because of its outstanding photocatalytic activity, long-term stability, low cost, and nontoxicity [6, 7]. However, TiO_2 can only be activated with UV light with a wavelength of less than 385 nm due to its wide band gap (~3.2 eV), which limits its utilization of the solar energy. Therefore, a growing interest is also focused on the development of the new photocatalysts that can operate effectively under visible light irradiation. The doping of TiO_2 with foreign elements such as metals and nonmetals to improve the energy band structure of TiO_2 has been extensively investigated [8], and nitrogen doping TiO_2 has been demonstrated as a visible light photocatalyst [9]. However, the absorption edge of N-doped TiO_2 was just extended to the wavelength below 450 nm with a lower absorption constant. The non-TiO_2-based photocatalysts with a larger absorption coefficient, such as Ta_3N_5 [10], $Ga_{1-x}Zn_xN_{1-x}O_x$ [11, 12], $BiVO_4$ [13, 14], Bi_2WO_6 [15, 16], and Ag_2CrO_4 [17] have also been studied during the past decade. Up to now, the development of novel visible-light-responsive photocatalysts with expanded spectral response range and high photocatalysis quantum efficiency is still necessary.

Recently, Yi et al. reported the new use of Ag_3PO_4 semiconductor as a visible light photocatalyst, which can oxidize water as well as decompose organic contaminants in aqueous solution [18]. It was found that it exhibited extremely high photocatalytic efficiency for organic dye decomposition under visible light irradiation and the decomposition of methylene blue over Ag_3PO_4 was dozens of times quicker than that over monoclinic $BiVO_4$ and commercial $TiO_{2-x}N_x$. However, the effect about reducing the crystallite size of Ag_3PO_4 on photocatalysis is still unknown.

Layered double hydroxide (LDH), also called hydrotalcite-like compound or anionic clay, is a family of lamellar ionic solids that in terms of layer charge are the counterpart of cationic clay minerals [19]. The LDH has a unique property known as "memory effect," which refers to that LDH is decomposed into mixed metal oxide (MMO) when LDH calcined at 300–600°C. The calcined LDH is able to recover the original layered structure easily when exposed to the air or put into anion aqueous solution [4, 20]. In our previous work, we have prepared flaky layered double

hydroxides (FLDH) composed of cross-linked nanoflakes by the reconstruction of their oxides in alkali solution, and the ZnO immobilized on FLDH generated highly dispersed ZnO nanoparticles (~9.5 nm in diameter) with an enhanced photocatalytic efficiency [21]. Nevertheless, the band gap of this composite (~3.18 eV) is too wide to absorb sunlight efficiently. In this work, we synthesized the Ag_3PO_4/FLDH composites, and the much finer Ag_3PO_4 was obtained in the presence of FLDH and the resulted composites exhibited a higher visible light photocatalytic efficiency compared to bare Ag_3PO_4.

2. Experimental

2.1. Synthesis of Materials. The Mg-Al-CO_3 LDH was prepared by coprecipitation by a high supersaturation method [22]. A typical preparation process was described as follows. Solution A was prepared by dissolving $AlCl_3 \cdot 6H_2O$ (62.5 mmoL) and $MgCl_2 \cdot 6H_2O$ (125 mmoL) in 87.5 mL of deionized water and solution B prepared via dissolving NaOH (437 mmoL) and Na_2CO_3 (208 mmoL) in 125 mL of deionized water. Solution A was added to solution B in a three-neck round-bottom reaction flask and then stirred at 50°C, subsequently heated to 90°C for 4 h. LDH was obtained after collection of the precipitates by filtration, washing several times with distilled water, and drying at 90°C overnight.

FLDH was prepared by the reconstruction of its oxide in alkali solution [21]. Firstly, LDH was calcined in air at 500°C for 4 h, with a heating rate of 4°C/min, to prepare the MMO. Secondly, 3.0 g MMO was dispersed into 200 mL 1.0 M Na_2CO_3 solution and stirred for 5 min; the suspension was then transferred into a temperature-humidity chamber and stirred for 24 h at 6°C. FLDH was obtained after collection of the precipitates by filtration, washing several times with distilled water, and drying at 90°C overnight.

The Ag_3PO_4/FLDH composites were prepared as follows. 3.0 g FLDH mixed with 4.8 g Na_2HPO_4 was placed into 150 mL of the distilled water under room temperature and stirred for 5 min. A proper amount of $AgNO_3$ was dissolved in 50 mL of the distilled water and added to the suspension above. After stirring vigorously for 20 min at room temperature, the suspension was filtered, washed several times with distilled water, and dried at 60°C overnight. By varying the amount of $AgNO_3$, the composites with Ag_3PO_4/FLDH mass ratios at 1 : 1.6 and 1 : 3 (labeled Ag_3PO_4/FLDH-1.6 and Ag_3PO_4/FLDH-3, resp.) were prepared. Bare Ag_3PO_4 sample without FLDH was also prepared by a similar method.

2.2. Characterization. The X-ray diffraction (XRD) patterns of the powder phase compositions were identified by X-ray diffractometer (Model D/Max-2550, Rigaku Co., Japan) using Cu K_α irradiation (λ = 1.5406 Å) at 40 kV and 100 mA. The size and morphology of the samples were determined by field emission scanning electron microscopy (FE-SEM) (Model S-4800, Hitachi, Japan) and transmission electron microscope (TEM) (Model JEM-2100F, JEOL, Japan). The Brunauer-Emmett-Teller (BET) specific surface area measurement and the Barrett-Joyner-Halenda (BJH) pore volume were performed using a nitrogen adsorption apparatus (Model Autosorb-1MP, Quantachrome Instruments Co., USA). The UV-vis diffuse reflectance spectra of the powder samples were collected in the form of a dry-pressed disk at room temperature with a spectrophotometer (Model Lambda 950, Perkin-Elmer Co., USA).

2.3. Photocatalytic Tests. Photocatalytic activities of the resultant bare Ag_3PO_4 and Ag_3PO_4/FLDH composites were evaluated by the photocatalytic decomposition of acid red G (ARG) under visible light irradiation. A 500 W Xe lamp was used as the light source, and a ZJB 420 filter glass was used to cut off light of wavelength <420 nm. In view of the fact that Ag_3PO_4 was slightly soluble in aqueous solution [23], the amount of catalysts in every experiment was normalized by the mass of Ag_3PO_4 really present in each sample and made sure that the amount of Ag_3PO_4 in ARG solution equal to 1 g/L. The experiments were performed as follows. Amount of photocatalyst was added into 100 mL ARG (50 mg/L). The aqueous suspension was stirred at room temperature and irradiated with visible light. About 3 mL of reaction suspension was sucked at a defined time interval, and the solid material was separated by centrifugation. The removal rates of ARG were measured on a UV-vis spectrophotometer (Model Lambda 35, Perkin-Elmer Co., USA) at the wavelength of 530 nm.

3. Results and Discussion

3.1. Characterization. Figure 1 shows the XRD patterns of the original LDH, MMO, and FLDH. The typical X-ray pattern of the original LDH (Figure 1(a)) exhibits the typical reflections of Mg-Al-CO_3-LDH with a series of narrow, symmetric, and sharp peaks, indicating a high degree of crystallinity [24]. Calcination of the LDH at 500°C resulted in the formation of a mixed metal oxide phase with an MgO-like structure (Figure 1(b)). After regeneration by soaking the MMO into a Na_2CO_3 solution, the calcined LDH have successfully recovered the original layered structure according to the characteristic reflections corresponding to the original LDH (Figure 1(c)), though a loss of some degree of crystallinity as reported elsewhere [25].

The XRD patterns of bare Ag_3PO_4, Ag_3PO_4/FLDH-1.6, and Ag_3PO_4/FLDH-3 are shown in Figure 2. For bare Ag_3PO_4 (Figure 2(a)), all of the diffraction peaks are well indexed as the body-centered cubic Ag_3PO_4 (JCPDS No. 06-0505). For the Ag_3PO_4/FLDH composites (Figures 2(b) and 2(c)), most of the diffraction peaks could be attributed to the body-centered cubic Ag_3PO_4. Meanwhile, small diffraction peaks of LDH have been detected just as that in Figure 1(c), confirming that the FLDH preserve its original structure after being coated with Ag_3PO_4.

The FE-SEM images in Figure 3 show the morphologies of LDH and FLDH. Figure 3(a) shows the plate-like morphology typical of LDH [26] with diameters in the range 50–100 nm. After regeneration, as shown in Figure 3(b), FLDH is made up of flaky sheets coalesced irregularly with each other.

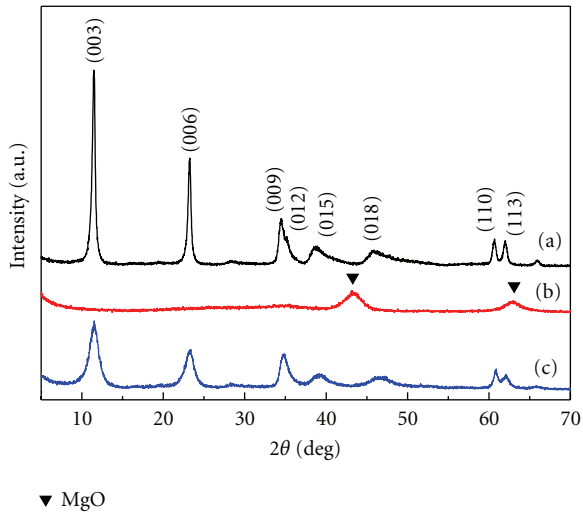

Figure 1: XRD patterns of (a) the original LDH, (b) MMO, and (c) FLDH.

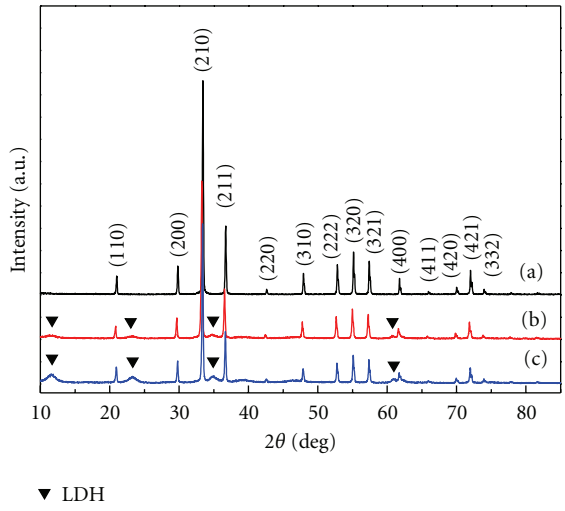

Figure 2: XRD patterns of (a) bare Ag_3PO_4, (b) Ag_3PO_4/FLDH-1.6, and (c) Ag_3PO_4/FLDH-3.

The sizes of the flaky sheets range from 50 to 200 nm, and the thickness is ~10 nm. It means that these sheets have a large aspect ratio (defined as platelet diameter/thickness) which may lead to an efficient adsorption capability.

The TEM images in Figure 4 show the sizes and morphologies of Ag_3PO_4 and Ag_3PO_4/FLDH-3. The TEM image of bare Ag_3PO_4 shows agglomerated particles with diameters in the range 200–1000 nm (Figure 4(a)). The average diameter of the well-distributed Ag_3PO_4 in the Ag_3PO_4/FLDH-3 composite (~200 nm) is smaller than that of the bare Ag_3PO_4 (Figure 4(a)). From these results, it can be concluded that FLDH plays an important role in hindering the crystal growth and agglomeration of Ag_3PO_4. Figure 4(c) shows the energy dispersive spectroscopy (EDS) pattern of Ag_3PO_4/FLDH-3. Except for the Cu and C peaks coming from the copper grid for the TEM analysis, the Mg and Al peaks are

Table 1: Corresponding specific surface area and pore volume for the samples.

Sample	S^a_{BET} (m^2/g)	V^b (cm^3/g)
LDH	110.4	0.336
FLDH	146.4	0.769
Ag_3PO_4	1.6	0.002
Ag_3PO_4/FLDH-1.6	106.1	0.495
Ag_3PO_4/FLDH-3	122.3	0.601

[a]BET surface area determined by a multipoint BET method, using the adsorption data in the relative pressure ($P/P0$) range 0.05–0.3. [b]BJH pore volume determined by the volume of nitrogen adsorbed at a relative pressure ($P/P0$) of 0.994.

corresponding to FLDH, and the presence of Ag and P elements indicates the formation of Ag_3PO_4. This result confirms that Ag_3PO_4/FLDH composites were successfully prepared in this study.

The BET specific surface area and pore volume of the samples are summarized in Table 1. It can be seen that the original LDH has a BET surface area 110.4 m^2/g with a relative lower pore volume 0.336 cm^3/g. After regeneration, the BET specific surface area and pore volume of FLDH are much larger than that of LDH, this may be because the newly formed FLDH has a coarse surface due to the irregular interconnected nanosheets and the remaining slit-like mesopores as shown in Figure 3(b) [21]. This higher surface area and the special structure are considered to be a suitable support for Ag_3PO_4 dispersion. The surface area of Ag_3PO_4/FLDH-1.6, and Ag_3PO_4/FLDH-3 are slightly lower than that of FLDH and decrease with increasing the Ag_3PO_4/FLDH mass ratios. This could be attributed to that the presence of Ag_3PO_4 can clog the pore of FLDH, and this effect is more and more significant with the amount of Ag_3PO_4, which is further confirmed by change in the pore volume. It can also be observed that the surface area and pore volume of bare Ag_3PO_4 are very low, which is expected to be responsible for the subsequent poor adsorption capacity of ARG.

The UV-vis diffuse reflectance spectra of the bare Ag_3PO_4, Ag_3PO_4/FLDH-1.6 and Ag_3PO_4/FLDH-3 are shown in Figure 5. It can be clearly seen that the bare Ag_3PO_4 can absorb solar energy with a wavelength shorter than ~530 nm as reported by Yi et al. [18]. As for Ag_3PO_4/FLDH composites, the absorption edge of each sample shifts to a slightly shorter wavelength compared with bare Ag_3PO_4 (~525 nm for Ag_3PO_4/FLDH-1.6 and ~520 nm for Ag_3PO_4/FLDH-3), though the absorption intensity slightly decreases. The decrease of absorption intensity is dependent on the content of Ag_3PO_4 in these composites.

3.2. Degradation of ARG Solution. The photocatalytic activity of Ag_3PO_4 may be explained by that Ag_3PO_4 has a large dispersion of conduction band due to the form of the delocalized π^* antibonding states in the conduction band and the inductive effect of PO_4^{3-}, which helps the separation of electron-hole pairs [27], and a strong oxidation of photoexcited holes in the valence band could be responsible for the dye degradation [18].

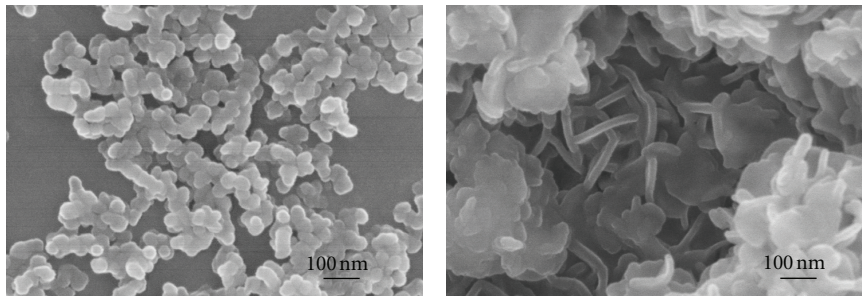

(a) (b)

Figure 3: SEM images of (a) LDH and (b) FLDH.

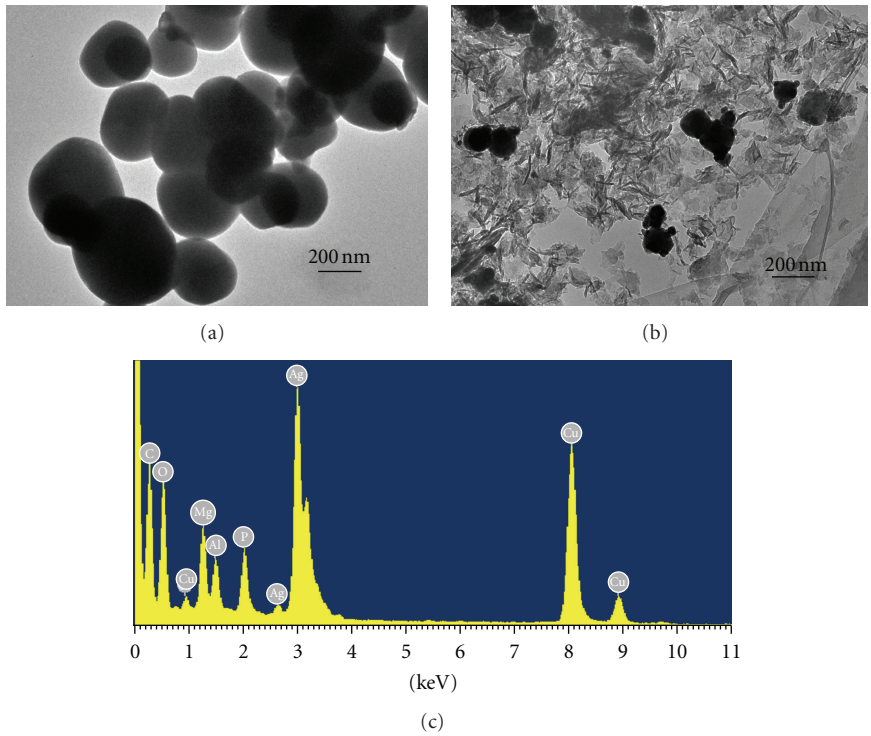

(a) (b) (c)

Figure 4: TEM images of Ag_3PO_4 (a) and Ag_3PO_4/FLDH-3 (b), and EDS elemental microanalysis of Ag_3PO_4/FLDH-3 (c).

The photocatalytic activities in decomposing ARG are plotted in Figure 6, where C_0 and C_t are the concentration of aqueous ARG in the starting aqueous (50 mg/L) and at time t, respectively. All of the samples showed efficient photocatalytic activities under visible light irradiation, indicating the potential of Ag_3PO_4 as a photofunctional material for waste water cleaning. It can be clearly seen that both of the Ag_3PO_4/FLDH photocatalysts exhibited higher photocatalytic activities for the ARG degradation reaction than bare Ag_3PO_4, especially Ag_3PO_4/FLDH-3, the ARG dye can be completely degraded within 20 min under visible light irradiation.

The enhanced photocatalytic properties can be attributed to two main factors. First is the much smaller size and good dispersion of Ag_3PO_4 immobilized on the FLDH. It is well known that the light-generated charge carriers in small-sized semiconductor grains can efficiently transfer to the surface, which results in the decrease of the opportunities for recombination [28]. Meanwhile, for bare Ag_3PO_4, the by-products, black metallic Ag particles, would appear because of the photocorrosion during the photocatalytic process and attach themselves onto the surface of the Ag_3PO_4 catalyst, which would inevitably prevent visible light absorption and decrease its photocatalytic activity [23]. For the Ag_3PO_4/FLDH composites, the photocorrosion still existed, but the Ag particles resulted from the decomposition of much finer Ag_3PO_4 in the composite were also much smaller compared to that from the bare Ag_3PO_4. The finer Ag particles scattered less light and improved the light harvesting in the photocatalytic process. Moreover, a large part of Ag particles would deposit onto the surface of FLDH not coated by Ag_3PO_4 in the composites, which also further reduce the negative influence. Second is a higher adsorption capability for the composites compared with bare Ag_3PO_4. The photocatalytic degradation

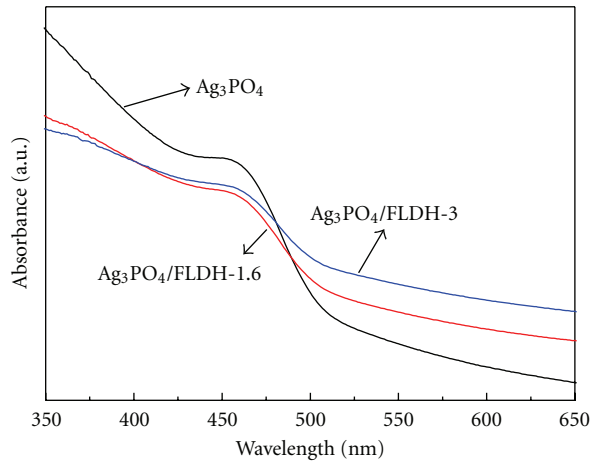

Figure 5: UV-vis diffuse reflectance spectra of bare Ag_3PO_4 and Ag_3PO_4/FLDH composites.

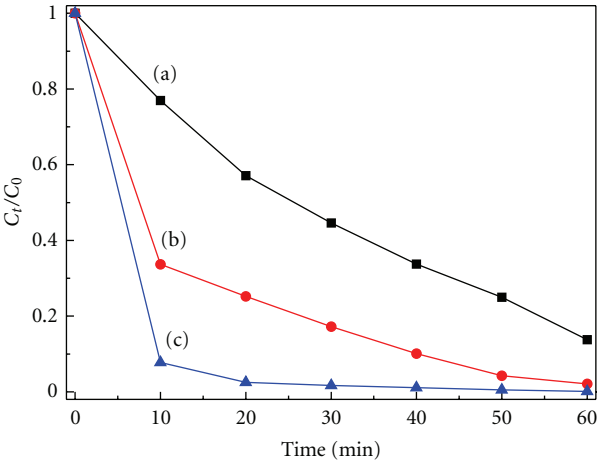

Figure 6: Photocatalytic activities of (a) Ag_3PO_4, (b) Ag_3PO_4/FLDH-1.6, and (c) Ag_3PO_4/FLDH-3 for ARG degradation under visible light irradiation.

of a pollutant must proceed at the surface of the catalyst after the reactant has been adsorbed on the surface, so the adsorption is considered to be the prestep for the consequent photocatalytic reaction [29]. According to the blank tests carried out like the way of photocatalytic degradation of ARG but without light irradiation, which are shown in Figure 7, it can be clearly seen that the adsorption of ARG on bare Ag_3PO_4 in the dark was negligible after 60 min, however, the percentages of ARG removal with Ag_3PO_4/FLDH-1.6 and Ag_3PO_4/FLDH-3 were ~35% and 55%, respectively. These results indicate that the high adsorption capability is very crucial to the improvement of photocatalytic activation for the Ag_3PO_4/FLDH composites. For Ag_3PO_4/FLDH-3, the excellent efficiency may be explained based on the smaller particle size, better dispersion of Ag_3PO_4 on the FLDH, and higher adsorption capability with the amount of FLDH content.

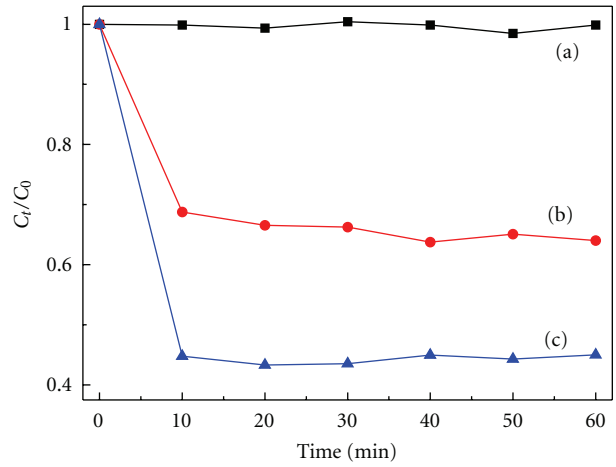

Figure 7: The adsorption capabilities of ARG on (a) Ag_3PO_4, (b) Ag_3PO_4/FLDH-1.6 and (c) Ag_3PO_4/FLDH-3 in the dark.

4. Conclusions

In summary, we synthesized the Ag_3PO_4/FLDH composites with fine Ag_3PO_4 crystalline grains through a wet chemical method. The Ag_3PO_4/FLDH composites, the Ag_3PO_4/FLDH-3 in particular, exhibited much higher catalytic efficiency than bare Ag_3PO_4 for the degradation of ARG under visible light irradiation. The enhanced photocatalytic properties can be attributed to the combination of the smaller-sized and well-distributed Ag_3PO_4 immobilized on the FLDH and the strong adsorption of the dye on the FLDH.

Acknowledgments

This work was supported by National Key Technology R&D Program (no. 2006BAA04B02-01) and Shanghai Leading Academic Discipline Project (B603).

References

[1] G. Li, D. Zhang, and J. C. Yu, "Ordered mesoporous $BiVO_4$ through nanocasting: a superior visible light-driven photocatalyst," *Chemistry of Materials*, vol. 20, no. 12, pp. 3983–3992, 2008.

[2] C. An, S. Peng, and Y. Sun, "Facile synthesis of sunlight-driven AgCl: Ag plasmonic nanophotocatalyst," *Advanced Materials*, vol. 22, no. 23, pp. 2570–2574, 2010.

[3] Z. Liu, H. Bai, and D. Sun, "Facile fabrication of hierarchical porous TiO_2 hollow microspheres with high photocatalytic activity for water purification," *Applied Catalysis B*, vol. 104, no. 3-4, pp. 234–238, 2011.

[4] S. Yuan, Y. Li, Q. Zhang, and H. Wang, "ZnO nanorods decorated calcined Mg-Al layered double hydroxides as photocatalysts with a high adsorptive capacity," *Colloids and Surfaces A*, vol. 348, no. 1–3, pp. 76–81, 2009.

[5] Q. Zhang, W. Fan, and L. Gao, "Anatase TiO_2 nanoparticles immobilized on ZnO tetrapods as a highly efficient and easily recyclable photocatalyst," *Applied Catalysis B*, vol. 76, no. 1-2, pp. 168–173, 2007.

[6] M. L. Chen and W. C. Oh, "The improved photocatalytic properties of methylene blue for V_2O_3/CNT/TiO_2 composite under visible light," *International Journal of Photoenergy*, vol. 2010, Article ID 264831, 5 pages, 2010.

[7] K. Lv, Q. Xiang, and J. Yu, "Effect of calcination temperature on morphology and photocatalytic activity of anatase TiO_2 nanosheets with exposed 001 facets," *Applied Catalysis B*, vol. 104, no. 3-4, pp. 275–281, 2011.

[8] G. Cao, Y. Li, Q. Zhang, and H. Wang, "Synthesis and characterization of La_2O_3/$TiO_{2-x}F_x$ and the visible light photocatalytic oxidation of 4-chlorophenol," *Journal of Hazardous Materials*, vol. 178, no. 1–3, pp. 440–449, 2010.

[9] Y. Wang, C. Feng, M. Zhang, J. Yang, and Z. Zhang, "Visible light active N-doped TiO_2 prepared from different precursors: origin of the visible light absorption and photoactivity," *Applied Catalysis B*, vol. 104, no. 3-4, pp. 268–274, 2011.

[10] Q. Zhang and L. Gao, "Ta_3N_5 nanoparticles with enhanced photocatalytic efficiency under visible light irradiation," *Langmuir*, vol. 20, no. 22, pp. 9821–9827, 2004.

[11] K. Maeda, K. Teramura, and Lu D. L., "Photocatalyst releasing hydrogen from water-enhancing catalytic performance holds promise for hydrogen production by water splitting in sunlight," *Nature*, vol. 440, no. 7082, p. 295, 2006.

[12] M. Yashima, H. Yamada, K. Maeda, and K. Domen, "Experimental visualization of covalent bonds and structural disorder in a gallium zinc oxynitride photocatalyst $(Ga_{1-x}Zn_x)(N_{1-x}O_x)$: origin of visible light absorption," *Chemical Communications*, vol. 46, no. 14, pp. 2379–2381, 2010.

[13] A. Kudo, K. Omori, and H. Kato, "A novel aqueous process for preparation of crystal form-controlled and highly crystalline $BiVO_4$ powder from layered vanadates at room temperature and its photocatalytic and photophysical properties," *Journal of the American Chemical Society*, vol. 121, no. 49, pp. 11459–11467, 1999.

[14] G. Xi and J. Ye, "Synthesis of bismuth vanadate nanoplates with exposed 001 facets and enhanced visible-light photocatalytic properties," *Chemical Communications*, vol. 46, no. 11, pp. 1893–1895, 2010.

[15] Z. Zhang, W. Wang, M. Shang, and W. Yin, "Low-temperature combustion synthesis of Bi_2WO_6 nanoparticles as a visible-light-driven photocatalyst," *Journal of Hazardous Materials*, vol. 177, no. 1–3, pp. 1013–1018, 2010.

[16] M. Shang, W. Wang, S. Sun, L. Zhou, and L. Zhang, "Bi_2WO_6 nanocrystals with high photocatalytic activities under visible light," *Journal of Physical Chemistry C*, vol. 112, no. 28, pp. 10407–10411, 2008.

[17] S. Ouyang, Z. Li, Z. Ouyang, T. Yu, J. Ye, and Z. Zou, "Correlation of crystal structures, electronic structures, and photocatalytic properties in a series of Ag-based oxides: $AgAlO_2$, $AgCrO_2$, and Ag_2CrO_4," *Journal of Physical Chemistry C*, vol. 112, no. 8, pp. 3134–3141, 2008.

[18] Z. Yi, J. Ye, N. Kikugawa et al., "An orthophosphate semiconductor with photooxidation properties under visible-light irradiation," *Nature Materials*, vol. 9, no. 7, pp. 559–564, 2010.

[19] T. Hibino and W. Jones, "New approach to the delamination of layered double hydroxides," *Journal of Materials Chemistry*, vol. 11, no. 5, pp. 1321–1323, 2001.

[20] K. Klemkaite, A. Khinsky, and A. Kareiva, "Reconstitution effect of Mg/Ni/Al layered double hydroxide," *Materials Letters*, vol. 65, no. 2, pp. 388–391, 2011.

[21] Y. Zhi, Y. Li, Q. Zhang, and H. Wang, "ZnO nanoparticles immobilized on flaky layered double hydroxides as photocatalysts with enhanced adsorptivity for removal of acid red G," *Langmuir*, vol. 26, no. 19, pp. 15546–15553, 2010.

[22] W. T. Reichle, "Synthesis of anionic clay minerals (mixed metal hydroxides, hydrotalcite)," *Solid State Ionics*, vol. 22, no. 1, pp. 135–141, 1986.

[23] Y. Bi, S. Ouyang, J. Cao, and J. Ye, "Facile synthesis of rhombic dodecahedral AgX/Ag_3PO_4 (X = Cl, Br, I) heterocrystals with enhanced photocatalytic properties and stabilities," *Physical Chemistry Chemical Physics*, vol. 13, no. 21, pp. 10071–10075, 2011.

[24] F. Millange, R. I. Walton, and D. O'Hare, "Time-resolved in situ X-ray diffraction study of the liquid-phase reconstructitm of Mg-Al-carboaate hydrotalcite-like compounds," *Journal of Materials Chemistry*, vol. 10, no. 7, pp. 1713–1720, 2000.

[25] F. R. Costa, A. Leuteritz, U. Wagenknecht, D. Jehnichen, L. Häußler, and G. Heinrich, "Intercalation of Mg-Al layered double hydroxide by anionic surfactants: preparation and characterization," *Applied Clay Science*, vol. 38, no. 3-4, pp. 153–164, 2008.

[26] L. Wang, X. Xu, D. G. Evans, X. Duan, and D. Li, "Synthesis and selective IR absorption properties of iminodiacetic-acid intercalated MgAl-layered double hydroxide," *Journal of Solid State Chemistry*, vol. 183, no. 5, pp. 1114–1119, 2010.

[27] X. Ma, B. Lu, D. Li, R. Shi, C. Pan, and Y. Zhu, "Origin of photocatalytic activation of silver orthophosphate from first-principles," *Journal of Physical Chemistry C*, vol. 115, no. 11, pp. 4680–4687, 2011.

[28] L. Zhang, W. Wang, J. Yang et al., "Sonochemical synthesis of nanocrystallite Bi_2O_3 as a visible-light-driven photocatalyst," *Applied Catalysis A*, vol. 308, pp. 105–110, 2006.

[29] J. Liu, M. Dong, S. Zuo, and Y. Yu, "Solvothermal preparation of TiO_2/montmorillonite and photocatalytic activity," *Applied Clay Science*, vol. 43, no. 2, pp. 156–159, 2009.